

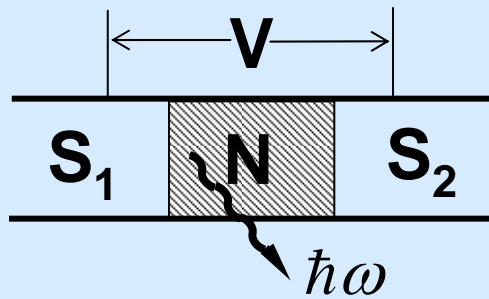
Low-temperature STM using the ac-Josephson Effect

Klaus Baberschke
Institut für Experimentalphysik
Freie Universität Berlin
Arnimallee 14 D-14195 Berlin-Dahlem
Germany

e-mail: bab@physik.fu-berlin.de
<http://www.physik.fu-berlin.de/~bab>

1. Introduction, single electron (quasi particle) tunneling
2. Josephson effect = pair tunneling
3. Our ac Josephson spectroscopy (25 years ago)
4. Proposal for a new ac Josephson UHV-LT-STs
5. Coupled superconductors SIS, SNS

ac-Josephson Effect



$$\partial(\theta_2 - \theta_1)/\partial t = -2eV/\hbar$$

$$\hbar\omega = 2eV$$

$$483,6 \text{ MHz} \hat{=} 1\mu\text{V}$$

**ac-Josephson Effekt
as Microwave Generator
and I(V) Curve as Detektor.**

K. D. Bures PhD and PRL 1984

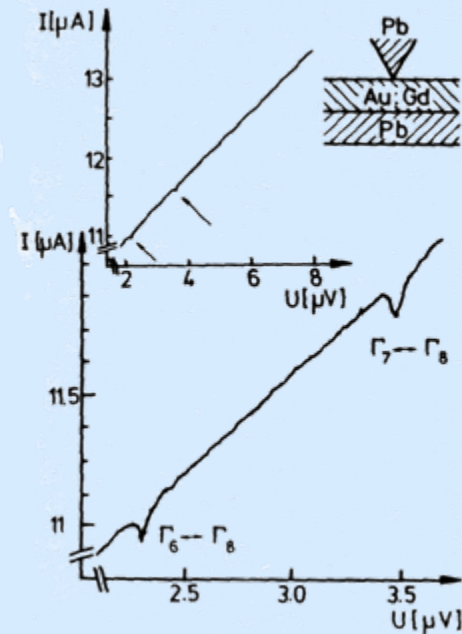
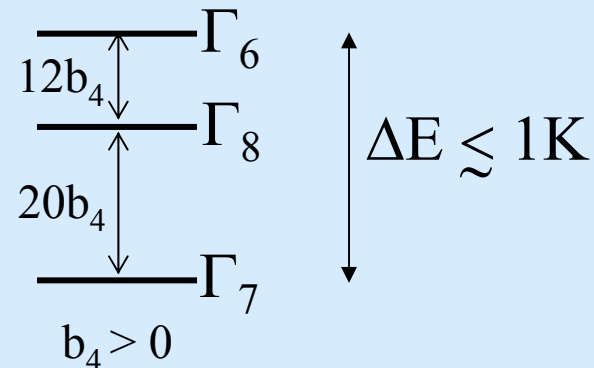


Fig. 5. Ausschnitte aus der I-V Charakteristik einer SNS Tunnelschicht. Resonanzen treten bei 2.26 und 3.42 μV auf.

$\text{Gd}^{3+} \text{ } ^8\text{S}_{7/2}$ in fcc Au



Coupled superconductors SIS, SNS

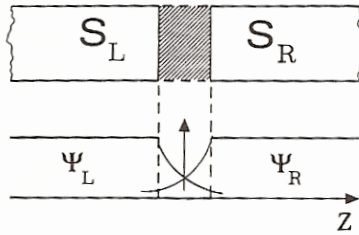


Figure 1.5 Schematic of a Josephson junction. S_L and S_R are the left and right superconductors. ψ_L and ψ_R are the left and right pair wavefunctions.

with the Hamiltonian given by

$$\mathcal{H} = \mathcal{H}_L + \mathcal{H}_R + \mathcal{H}_T$$

where $\mathcal{H}_L = E_L |L\rangle \langle L|$ and $\mathcal{H}_R = E_R |R\rangle \langle R|$ are relative to the unperturbed states $|L\rangle$ and $|R\rangle$.

$$\mathcal{H}_T = K [|L\rangle \langle R| + |R\rangle \langle L|]$$

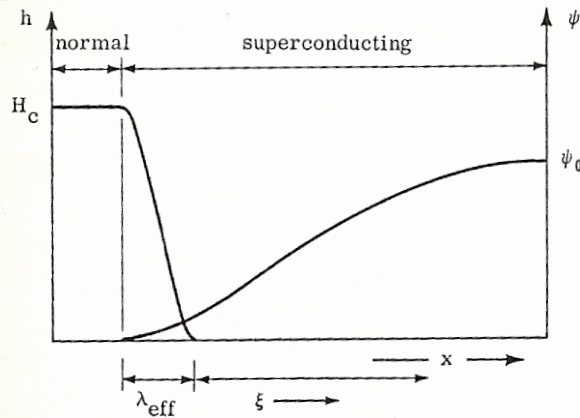


Figure 6-1

Spatial variation of the field and order parameter near a N-S wall for $\xi(T) \gg \lambda(T)$. The effective penetration depth λ_{eff} is of order $\sqrt{\lambda \xi}$ (see problem, page 178).

$$|\Psi_{L,R}|^2 = \rho, \text{ Cooper pair density order parameter}$$

Table 7-1
Characteristic Lengths

	Pure Metal	Dirty Metal
Range of the kernel $S_{\mu\gamma}$ (relation between current and vector potential)	$\xi_0 = 0.18 \frac{\hbar v_F}{k_B T_0}$	ℓ
Range of the kernel K_0 [self-consistency equation for $\Delta(\mathbf{r})$]	$\sim \xi_0$	$\sim \sqrt{\xi_0 \ell}$
Scale of the spatial variations of $ \Delta $ in the Landau-Ginsburg domain	$\xi(T) = 0.74 \xi_0 \left(\frac{T_0}{T_0 - T} \right)^{1/2}$	$\xi(T) = 0.85 \left(\frac{\xi_0 \ell T_0}{T_0 - T} \right)^{1/2}$
Penetration depth in the Landau-Ginsburg domain	$\lambda(T) = \frac{1}{\sqrt{2}} \lambda_L(0) \left(\frac{T_0}{T_0 - T} \right)^{1/2}$	$\lambda(T) = 0.64 \lambda_L(0) \left(\frac{\xi_0}{\ell} \frac{T_0}{T_0 - T} \right)^{1/2}$

Single electron tunneling (quasi particle t.)

$$2\Delta = 3.5 k_B T_C; \quad U \approx mV$$

$$10 \text{ K} \leftrightarrow 860 \mu eV$$

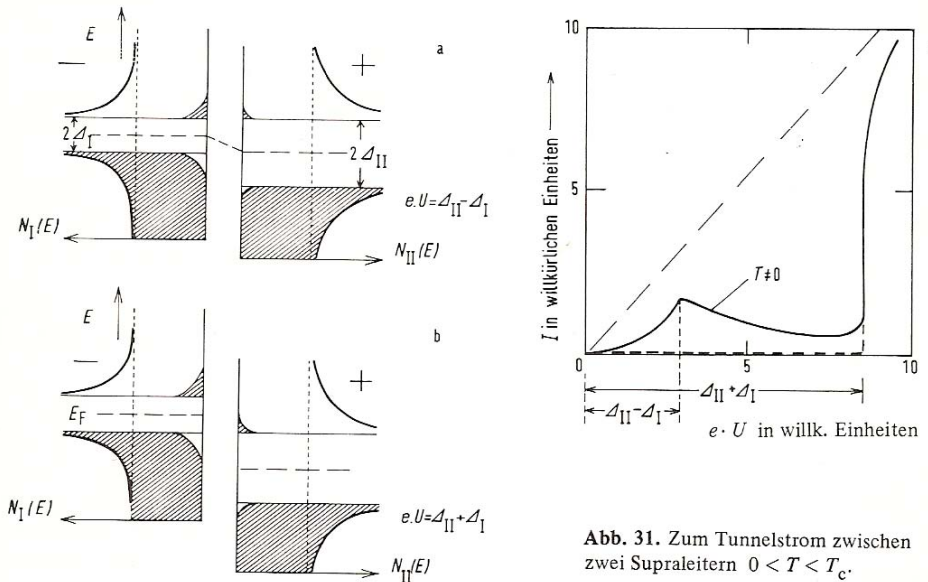


Abb. 31. Zum Tunnelstrom zwischen zwei Supraleitern $0 < T < T_c$.

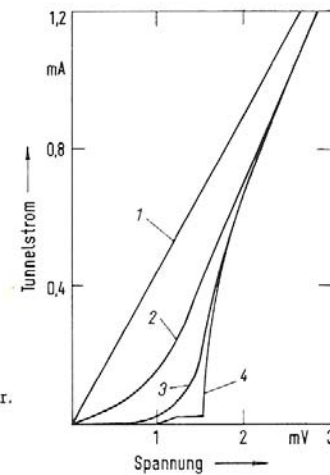
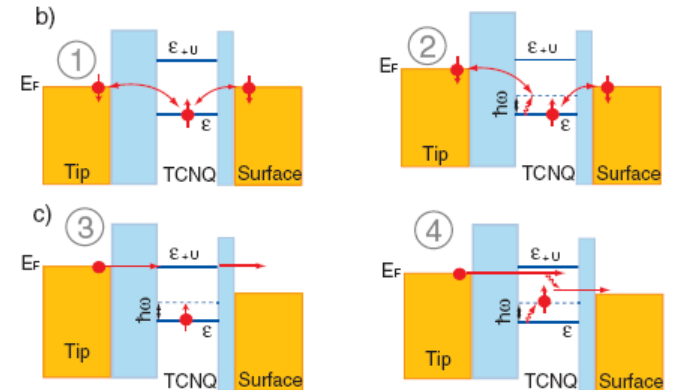
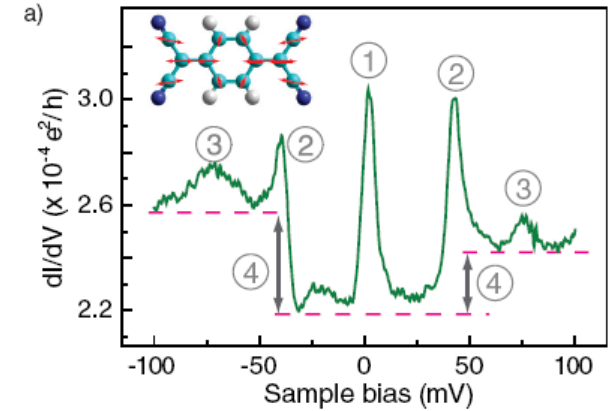


Abb. 33. Strom-Spannungs-Kennlinien eines Tunnelkontaktes Al-Al₂O₃-Pb, Registrierkurven. 1: $T = 10 \text{ K}$; 2: $T = 4,2 \text{ K}$; 3: $T = 1,64 \text{ K}$; 4: $T = 1,05 \text{ K}$; bei $1,05 \text{ K}$ ist auch das Al supra-leitend. Der steile Anstieg bei $eU = \Delta_I + \Delta_{II}$ ist deutlich sichtbar. Übergangstemperaturen: Pb $7,2 \text{ K}$; Al $1,2$ (nach [54]).



PRL 101, 217203 (2008)

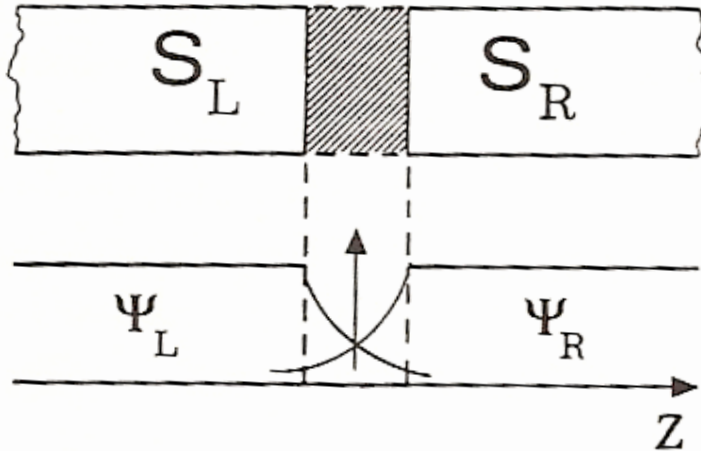
That's what we do NOT discuss

dc -Josephson effect = pair tunneling

Overlap of Ψ_L and Ψ_R . Ψ pair wave fct. leads to a tunnel current of Cooper pairs.

It's a new particle with $2e$, $2m$ and $S=0$ with Bose statistic.

Ψ is one macroscopic wave fct for all Cooper pairs.*



men wir an, daß beide auf dem Potential Null sind. Die zeitabhängige Schrödinger-Gleichung $i\hbar \partial \psi / \partial t = \mathcal{H} \psi$ auf beide Amplituden angewandt, ergibt

$$(38) \quad i\hbar \frac{\partial \psi_1}{\partial t} = \hbar T \psi_2 ; \quad i\hbar \frac{\partial \psi_2}{\partial t} = \hbar T \psi_1 .$$

Darin soll $\hbar T$ die Elektronenpaarkopplung oder Transfer-Wechselwirkung durch den Isolator beschreiben; T hat die Dimension einer Rate oder Frequenz. Es ist ein Maß für das Entweichen von ψ_1 in das Gebiet 2 und umgekehrt. Falls der Isolator sehr dick ist, wird T Null und es existiert kein Paar-Tunneln.

$$J_0 \hbar = 2T (\rho_L \rho_R)^{1/2}$$

Der Strom von 1 nach 2 ist proportional zu $\partial n_2 / \partial t$ oder, was das gleiche ist, proportional zu $-\partial n_1 / \partial t$. Wir schließen daher aus (43), daß der Strom J der supraleitenden Paare durch den Kontakt von der Phasendifferenz δ folgendermaßen abhängt:

$$(47) \quad J = J_0 \sin \delta = J_0 \sin (\theta_2 - \theta_1) ,$$

wobei J_0 proportional zur Transfer-Wechselwirkung T ist. Der Strom J_0 ist der größte Strom, der ohne Spannung durch die Kontaktschicht fließen kann. Ohne daß also eine Spannung angelegt wird, fließt ein Gleichstrom mit einem Wert zwischen J_0 und $-J_0$ durch den Kontakt, je nachdem wie groß die Phasendifferenz $\theta_2 - \theta_1$ ist. Das ist der Gleichstrom-Josephson-Effekt (Bild 24).

* This leads to flux quantization and Fresnel interference pattern

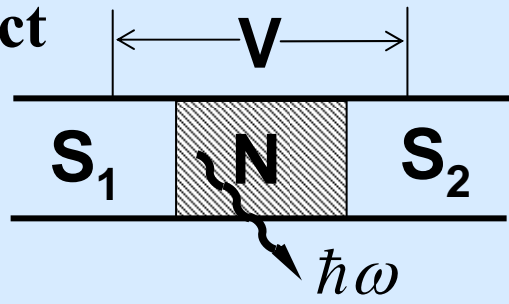
– not discussed today.

$$\Phi_0 = hc/2e \cong 2 \cdot 10^{-7} \text{ G} \cdot \text{cm}^2$$

Tunnel junction + voltage = ac Josephson effect

Wechselstrom-Josephson-Effekt. Über den Kontakt sei die Spannung V angelegt. Dies ist möglich, da die Kontaktschicht ja ein Isolator ist. Ein Elektronenpaar, das den Kontakt durchquert, spürt die Potentialdifferenz qV , wobei $q = -2e$. Wir können sagen, daß ein Paar auf der einen Seite die potentielle Energie $-eV$ und ein Paar auf der anderen Seite die potentielle Energie eV hat. Die Bewegungsgleichungen, die wir jetzt anstelle von (38) schreiben müssen, sind

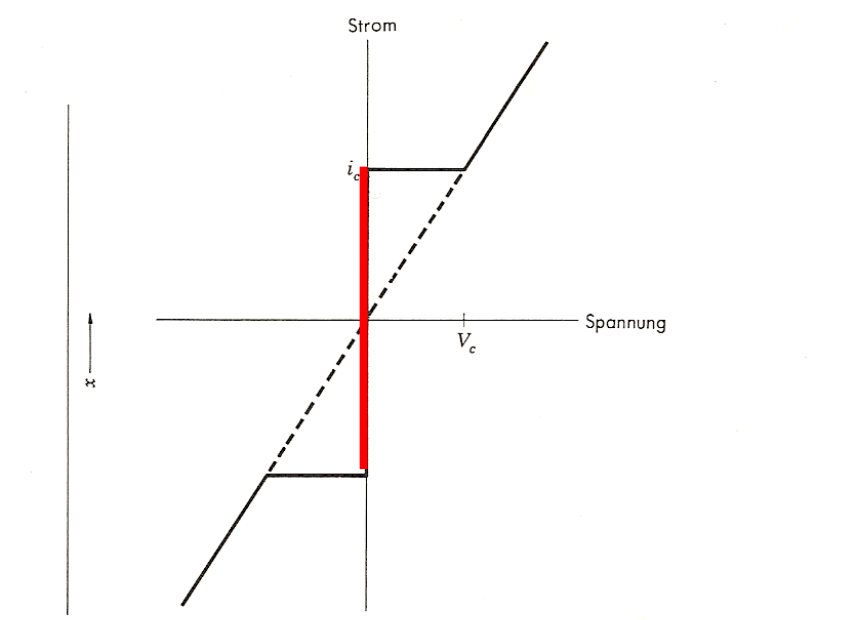
$$(48) \quad i\hbar \frac{\partial \psi_1}{\partial t} = \hbar T \psi_2 - eV \psi_1; \quad i\hbar \frac{\partial \psi_2}{\partial t} = \hbar T \psi_1 + eV \psi_2$$



$$J = J_0 \sin(\Delta\Theta - 2eVt/\hbar)$$

$$h\nu = 2eV$$

$$483.6 \text{ MHz} \leftrightarrow 1 \mu\text{V}$$



Strom-Spannungscharakteristik einer Josephson-Verbindung. Ohne angelegte Spannung fließen Gleichströme bis zu einem kritischen Strom der Stärke i_c : Das ist der DC-Josephson-Effekt. Bei Spannungen über V_c hat die Verbindung einen bestimmten Widerstand, der Strom hat jedoch einen oszillierenden Anteil mit der Frequenz $\omega = 2eV/\hbar$: Das ist der AC-Josephson-Effekt.

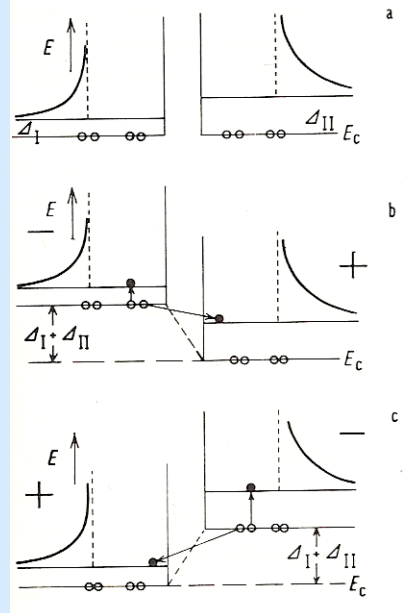


Abb. 36. Darstellung des Tunneleffektes zwischen Supraleitern im Bild der Cooper-Paare und der „angeregten“ Einzelelektronen. Cooper-Paare $\circ\circ$, Einzelelektronen (Anregungen) \bullet .

Our ac Josephson spectroscopy

VOLUME 53, NUMBER 1

PHYSICAL REVIEW LETTERS

2 JULY 1984

ESR *in Situ* with a Josephson Tunnel Junction

K. Baberschke and K. D. Bures

Institut für Atom- und Festkörperphysik, Freie Universität Berlin, D-1000 Berlin 33, Federal Republic of Germany

and

S. E. Barnes

Physics Department, University of Miami, Coral Gables, Florida 33124

(Received 3 April 1984)

The *in situ* electron-spin resonance of a voltage-biased NbAuNb Josephson junction is reported. The Au barrier is doped with Gd or ^{167}Er ions. Sharp resonances appear in the I - V curves at frequencies equivalent to the crystal-field splitting of AuGd (1.0 and 1.7 GHz) and to the hyperfine splitting of Au ^{167}Er (2.87 GHz). The principle of this new type of ESR-Josephson-junction spectrometer, as well as its application, is discussed.

ac-Josephson effect
as MW-generator
and current as detector

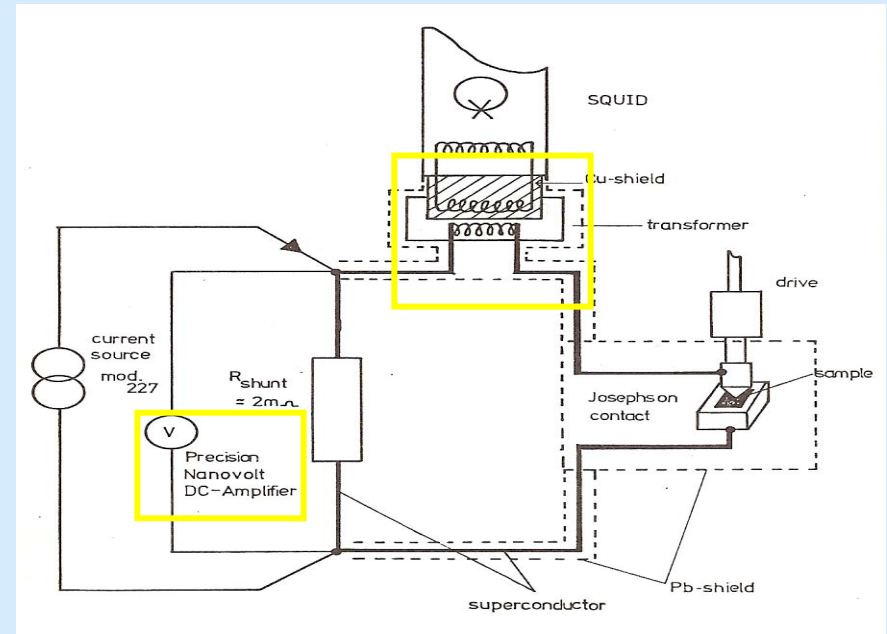


Abb. 2.1a

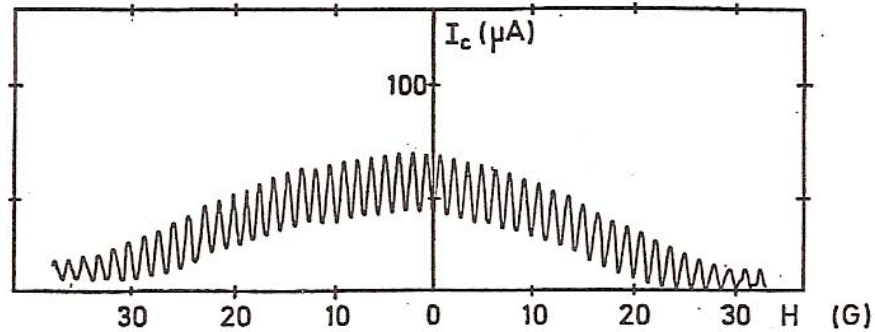


Abb. 2.1b

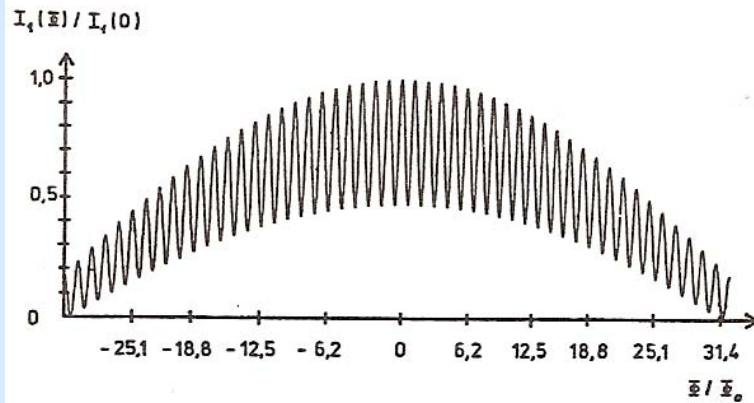
We worked with a tip and film thickness
of r and d of few μm , $R \approx 0.5 \Omega$



Proof for a good Josephson junction



$I_c(H)$ der Pr. 2 NbAuGdPb



Simulation

Apparative Empfindlichkeit (Stromquelle)

Stabilität der Stromkonstanter

$\pm(0,005\% \text{ pro Einstellung } \pm 0.005\% \text{ Bereich})/^\circ\text{C}$
 bei 1mA und Raumtemperatur ergibt sich:
 $I_N = \pm 50\text{nA}$



Lastregulierung

$\pm 0.005\%$ von Null nach Vollast
 Aufgrund des Verhältnisses von Zuleitungs R und R_N
 ergibt sich $\delta I/I \ll 10^{-10}$ Vernachlässigbar!



Experimentell ermittelte Stabilität

$I_N = \pm 15\text{nA}$
 bei gesteuertem Strom (0 bis 1mA in 6min)
 $\pm 1.5 \cdot 10^{-5}$ für den Bereich 1mA



Resultat: max. Rauschleistung $P_1 = 2 \cdot 10^{-13} \text{ W}$
 Frequenzmodulation ($2\text{m}\Omega, 2\mu\text{V}$) $\delta V/V = 5 \cdot 10^{-5}$

Spannungsrauschen

Nyquist-Rauschen

$\delta V/V = 1 \cdot 10^{-7}$
 $n_S = 3 \cdot 10^{-23} \text{ W}$
 vernachlässigbar



Thermospannung

$\delta V/V = 1 \cdot 10^{-3}$
 $2 \cdot \Delta T = 5 \cdot 10^{-15} \text{ W}$

$$n_S = 4kT\Delta\nu ; R_N = 2\text{m}\Omega$$

$$T = 4.2\text{K}; u_S = 6.8 \cdot 10^{-13}\text{V}$$

$$\text{Cu/Cu-Verb.} = \pm 0.25 \mu\text{V}/^\circ\text{C}$$

$$\Delta T = 10\text{mK}; \text{daraus } 2.5\text{nV}$$

Eigenrauschen des NVM

$$\delta V/V = 2 \cdot 10^{-3}$$

$$n_{\text{NVM}} = 5 \cdot 10^{-14} \text{ W}$$

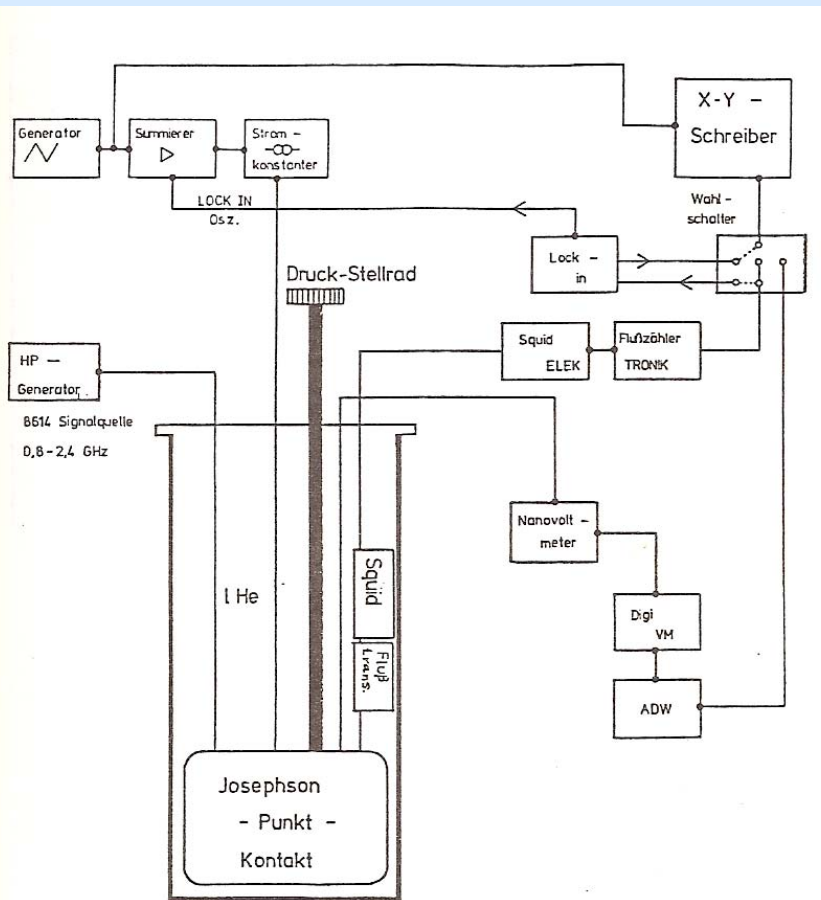


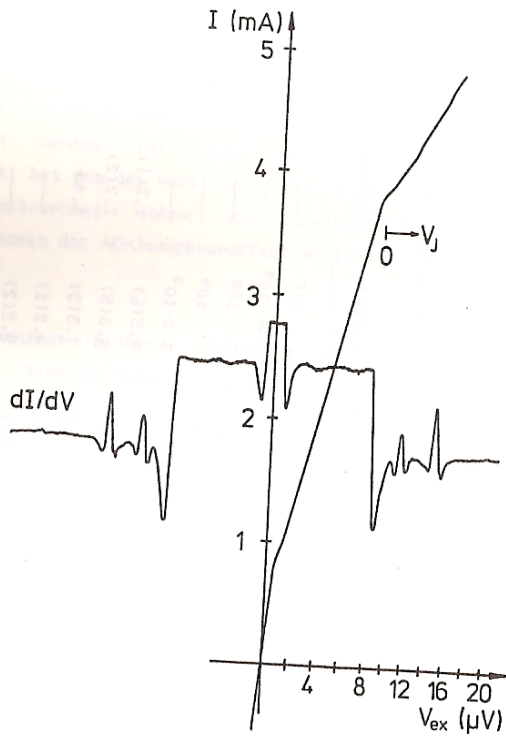
Eingangsrauschen:
 $u_a = 1 \cdot 10^{-5}\text{V}; \tau = 5\text{s}; R_N = 2\text{m}\Omega$
 Verstärkung 10^5

Der Beitrag ist vernachlässigbar, die beiden anderen ergeben:

$$\Delta E/E = 3 \cdot 10^{-3}$$

Die Auflösungsgrenze liegt damit bei $\Delta\nu \approx 5.8 \text{ MHz}$ ($\nu = 1\text{GHz}$)
 und ist durch das Rauschen des Nanovoltmeters bestimmt.





Kennlinie und Ableitung für Pr. 3 AuGd (500 ppm). Die Resonanzübergänge liegen bei $\nu_1=1.06(10)$ GHz, $\nu_2=1.66(7)$ GHz.

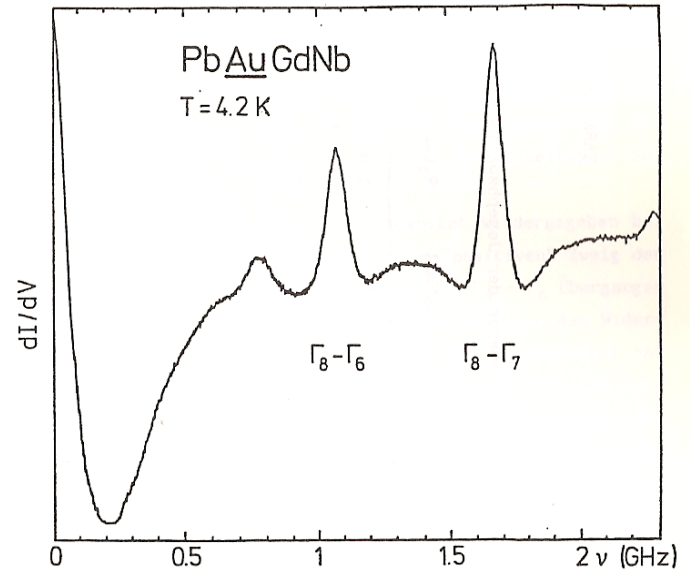


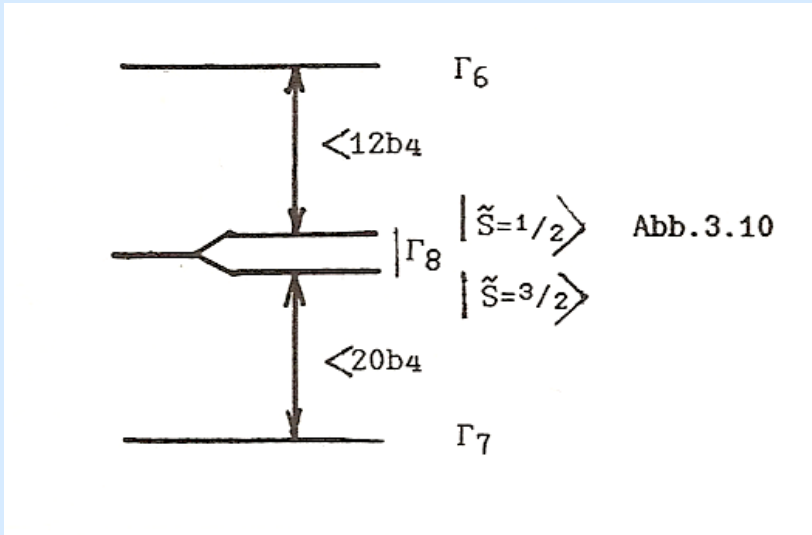
Abb. 3.6 Ableitung der Teilkennlinie aus Abb. 3.5

$$i_{tot} = \frac{V}{R} + \frac{i_c^2 R}{2V}$$

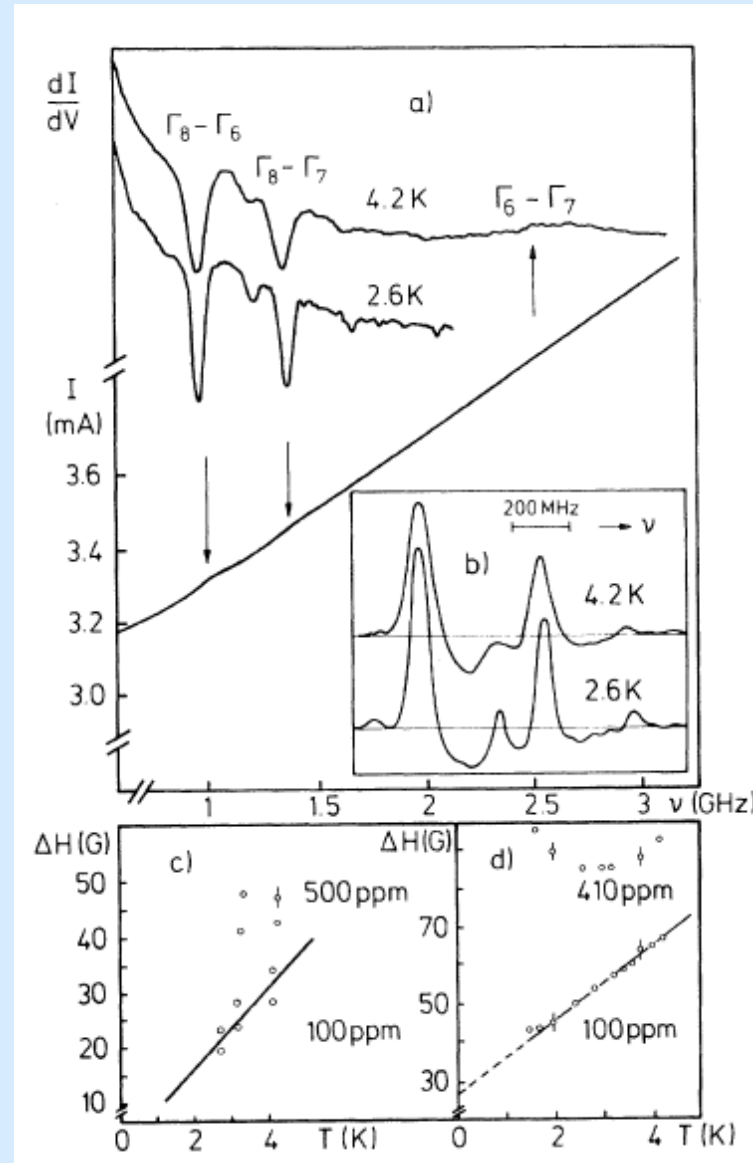
$$483,6 \text{ MHz} = 1 \mu\text{V}$$

$$\text{Gd}^{3+} \Rightarrow {}^8\text{S}_{7/2} \Rightarrow 2S+1 = 8$$

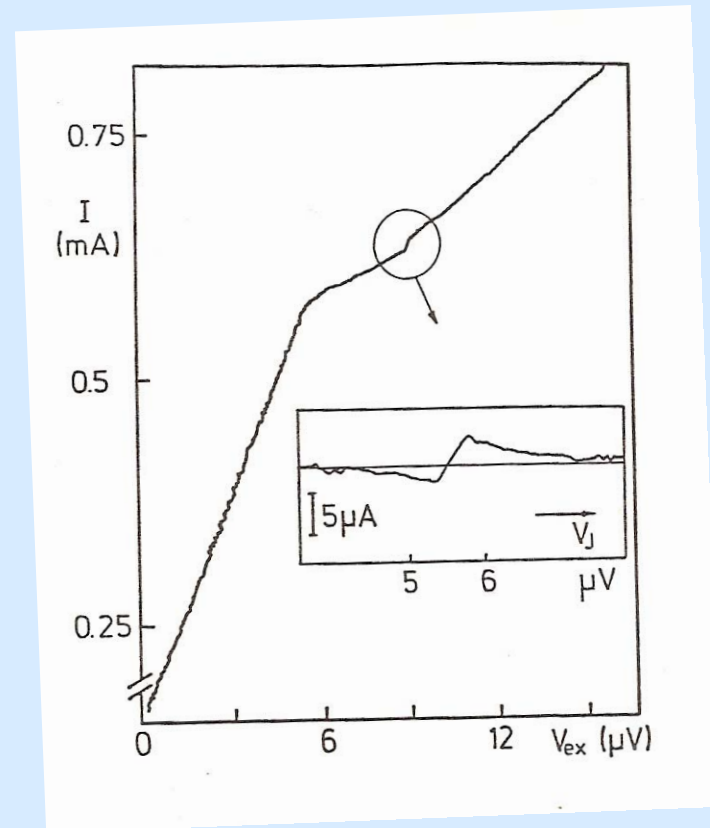
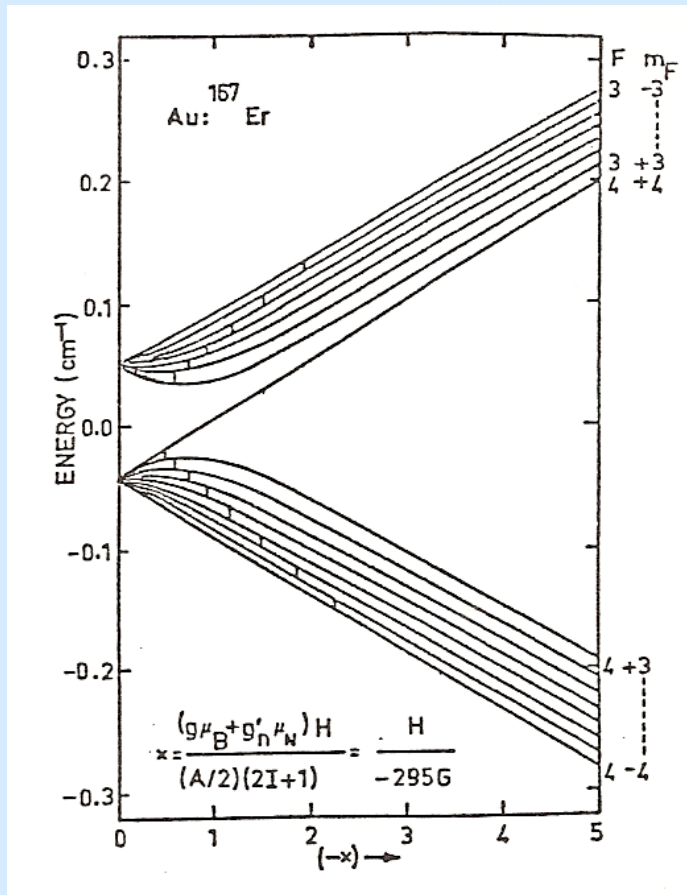
Crystal field splitting



cubic or lower symmetry



Hyperfine splitting of Au ^{167}Er , $S + I = F = 3$ and 4



$$\Delta E_{\text{theo}} = 2.87 \text{ GHz} ;$$

$$V_{\text{res}} = 5.4(2) \mu\text{V}, \quad \nu_{\text{res}} = 2.6(1) \text{ GHz}$$



DEPARTMENT OF PHYSICS, B-019
LA JOLLA, CALIFORNIA 92093

July 16, 1984

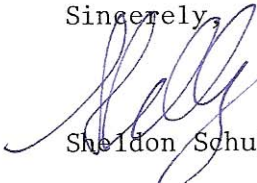
Professor Klaus Baberschke
Freie Universitat Berlin
Fachbereich Physik
Institut fur Atom-und Festkorperphysik (WE-1)
Arnimallee 14
1000 Berlin 33
Federal Republic of Germany

Dear Klaus:

I just saw your Physical Review Letter on esr using the Josephson structure and I can not resist writing to just say it sounds beautiful!

I look forward to discussing your results when I visit.

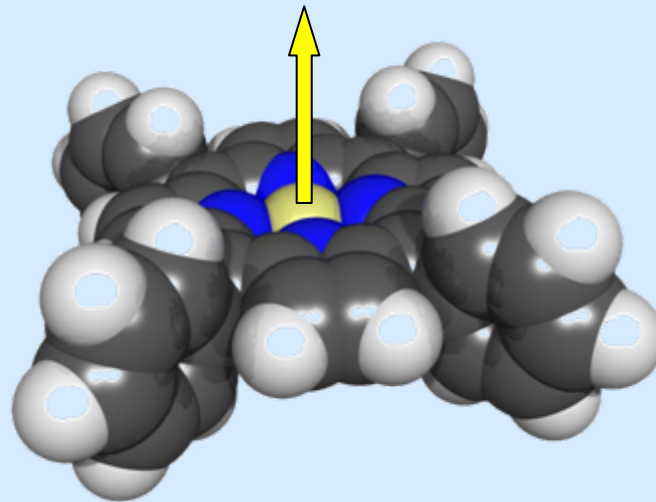
Sincerely,



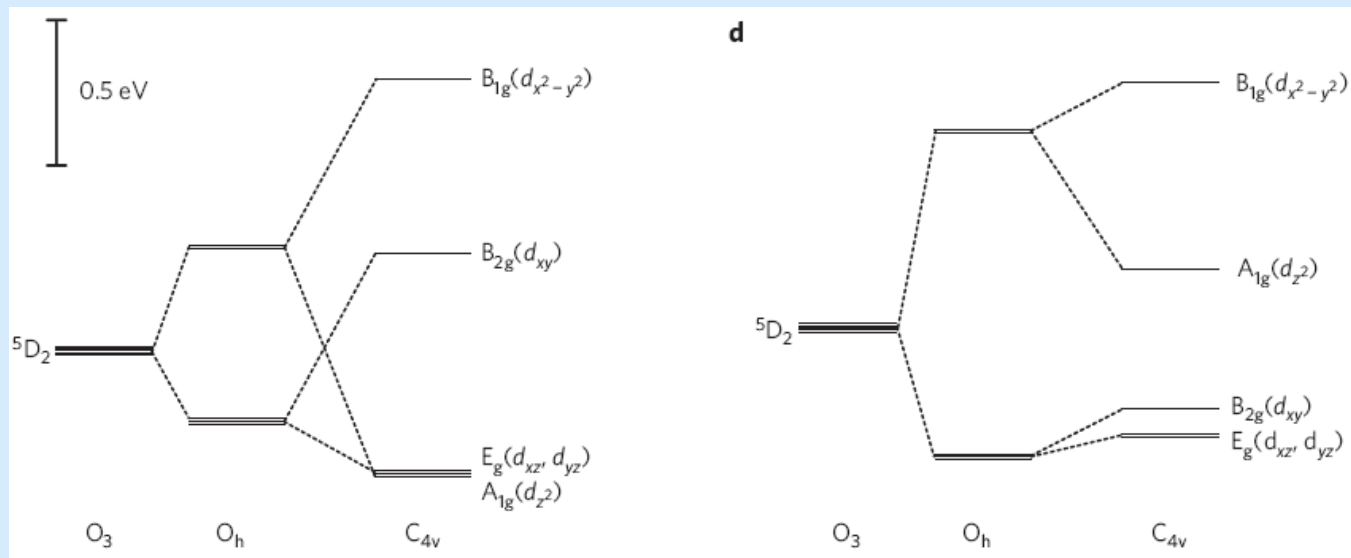
Sheldon Schultz

New ac Josephson UHV-LT-STM

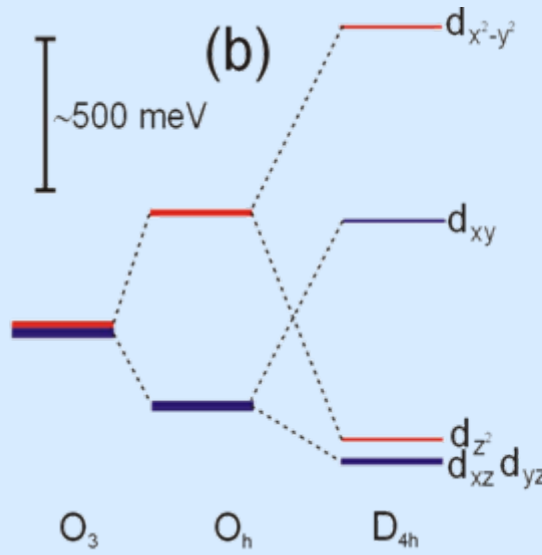
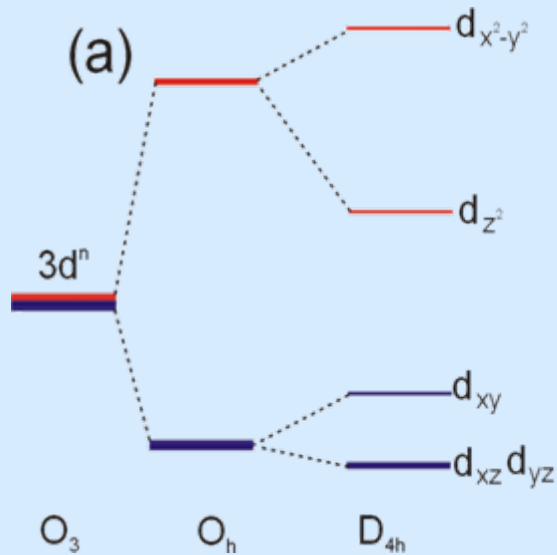
Fe^{3+} $S=5/2$



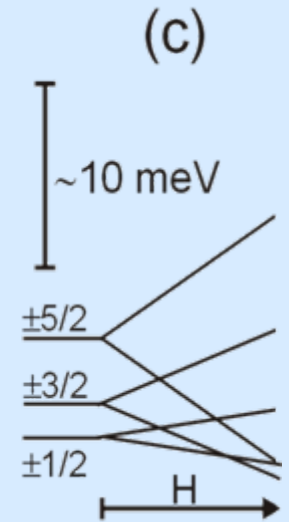
Fe^{3+} or Fe^{2+} ,
HS or LS,
finally there will be
some ZFS within
the $(2S+1)$ manifold



$3d^n$ -energy scheme and magnetism of the Fe-ion



Fe $3+, 2+$
 $S = 5/2, 3/2, 1/2$
 $S = 2, 1, 0$



Dramatic change of ligand field upon coadsorption of oxygen.

Gambardella et al. 2009,

Bernien et al. 2009

Unperturbed e_g, t_{2g} eigenstates are no good.

“zero field splitting” \equiv CEF

Für einen $3d^1$ Zustand mit MX_6 Liganden ist die Energieaufspaltung in tetragonaler Symmetrie wie folgt gegeben:

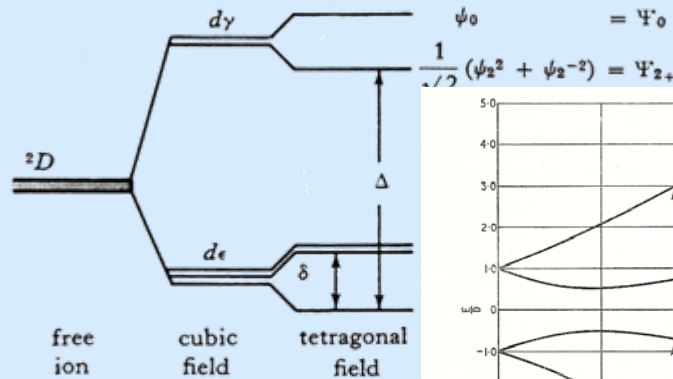


Fig. 3-4 Splitting of the 2D term by a tetragonal field

3) Berechnen Sie für den Grundzustand

$$\psi_{2-} = (2)^{-1/2} \{ |2> - |2-> \}$$

die Beimischung der angeregten Zustände durch die Spinzustände einzuführen sind (zweckmäßig $\alpha|2->$ und $\beta|2->$ für Spin "up" and "down")

(2 P)

4.) Berechnen Sie für den in Ü3 gefundenen neuen Grundzustand die anisotropen g-Faktoren

$g_x, g_y = g_z$ durch "Einschalten" der Zeeman Ww: $\mu_B(L+g_zS)H$

(3 P)

$$\mathcal{H}_s = \beta H(g_{\parallel} \cos \theta S_z + g_{\perp} \sin \theta S_x) + D(S_z^2 - \frac{1}{3}S(S+1)) \quad (4.10)$$

with $S = \frac{3}{2}$; where, as above, H is applied at an angle θ to the z axis in the zx plane.

The operator S_z^2 is diagonal, so in zero magnetic field it is easy to see that the eigenvalues of Equation 4.10 are

$$\begin{aligned} E_{\pm\frac{1}{2}} &= -D \\ E_{\pm\frac{3}{2}} &= +D \end{aligned} \quad (4.11)$$

i.e. the zero field splitting is $2D$. For

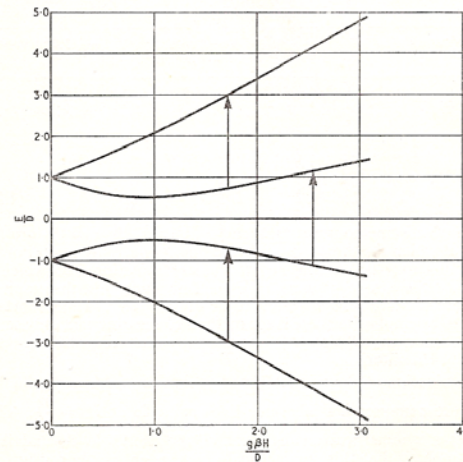


Fig. 4.1. "Symmetrical" energy levels for the system $S = \frac{3}{2}$ in axial crystal field. The magnetic field H is applied at an angle $\cos^{-1}(1/\sqrt{3})$ ($54^\circ 44'$) to the crystalline axis

Zero field splitting:

For $Cr^{3+} \Rightarrow S=3/2$, see FP

For $Fe^{3+} \Rightarrow S=5/2$

Splitting in $E_{\pm 1/2}, E_{\pm 3/2}, E_{\pm 5/2}$

$$\Delta E = 2D, \quad 4D$$

Range 5 to 40 GHz, see Bittl group

Introduction

20110 Ü

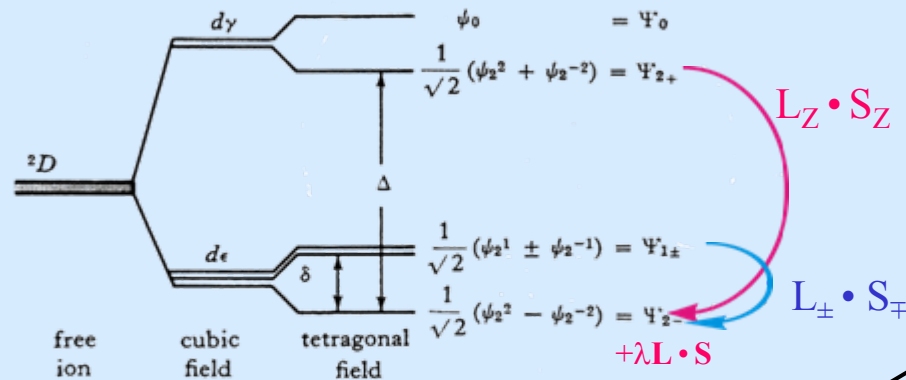
Übung zur Festkörperphysik II

SS 1998
Baberschke
Farle
Bovensiepen

Ausgabe: 28.0498

Abgabe: 08.05.98

Für einen $3d^1$ Zustand mit MX_6 Liganden ist die Energieaufspaltung in tetragonaler Symmetrie wie folgt gegeben:



The orbital moment is quenched in cubic symmetry

$$\langle 2- | L_z | 2- \rangle = 0,$$

but not for tetragonal symmetry

Fig. 3-4 Splitting of the 2D term by a tetragonally distorted cubic field.

3) Berechnen Sie für den Grundzustand

$$\psi_{2-} = (2)^{-1/2} \{ |2\rangle - |-2\rangle \} = |2-\rangle$$

die Beimischung der angeregten Zustände durch $\lambda \mathbf{L} \cdot \mathbf{S}$ und beachten Sie dabei, daß auch Spinzustände einzuführen sind (zweckmäßig $\alpha|2-\rangle$ und $\beta|2-\rangle$ für Spin "up" and "down")

(2 P)

4.) Berechnen Sie für den in Ü3 gefundenen neuen Grundzustand die anisotropen g-Faktoren

$g_x, g_y = g_z$ durch "Einschalten" der Zeeman Ww: $\mu_B (\mathbf{L} + g_s \mathbf{S}) \mathbf{H}$

(3 P)

Probing Superexchange Interaction in Molecular Magnets by Spin-Flip Spectroscopy and Microscopy

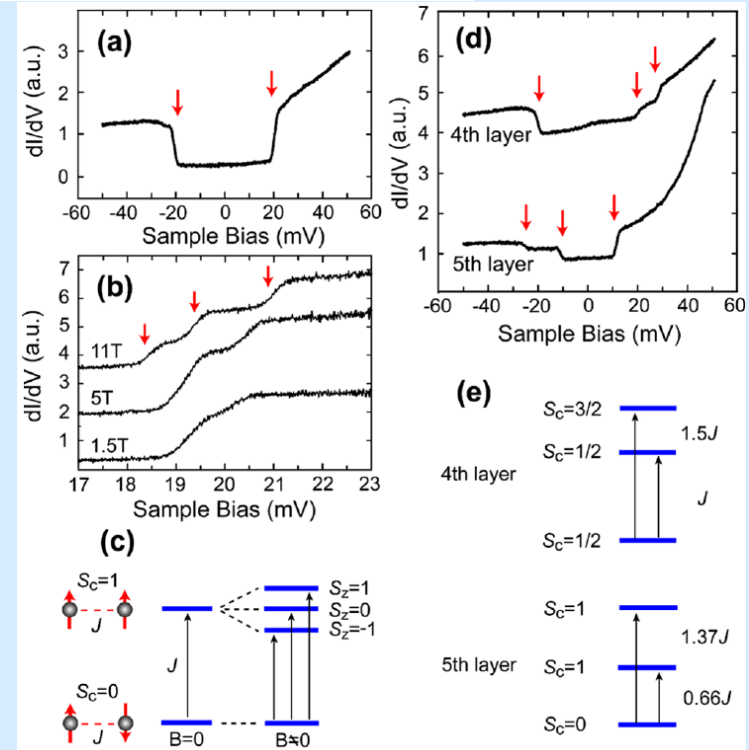
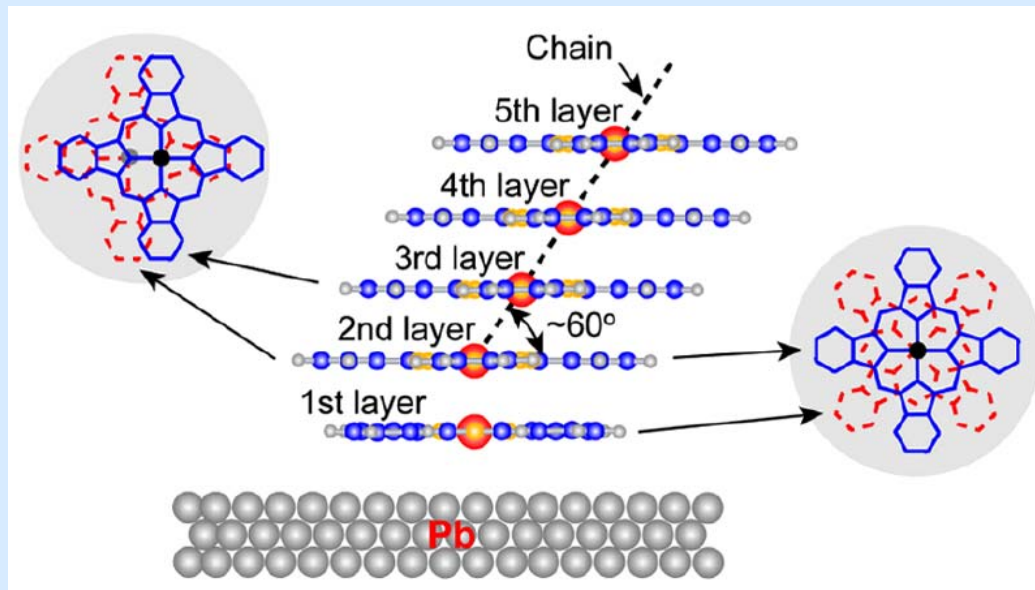
Xi Chen,¹ Ying-Shuang Fu,^{1,2} Shuai-Hua Ji,^{1,2} Tong Zhang,^{1,2} Peng Cheng,¹ Xu-Cun Ma,² Xiao-Long Zou,¹
Wen-Hui Duan,¹ Jin-Feng Jia,¹ and Qi-Kun Xue^{1,2,*}

¹Department of Physics, Tsinghua University, Beijing 100084, China

²Institute of Physics, Chinese Academy of Sciences, Beijing 100080, China

(Received 8 August 2008; published 7 November 2008)

The superexchange mechanism in cobalt phthalocyanine (CoPc) thin films was studied by a low temperature scanning tunneling microscope. The CoPc molecules were found to form one-dimensional antiferromagnetic chains in the film. Collective spin excitations in individual molecular chains were measured with spin-flip associated inelastic electron tunneling spectroscopy. By spatially mapping the spin-flipping channels with submolecular precision, we are able to explicitly identify the specific molecular orbitals that mediate the superexchange interaction between molecules.



Fluctuation Dominated Josephson Tunneling with a Scanning Tunneling Microscope

O. Naaman, W. Teizer, and R. C. Dynes*

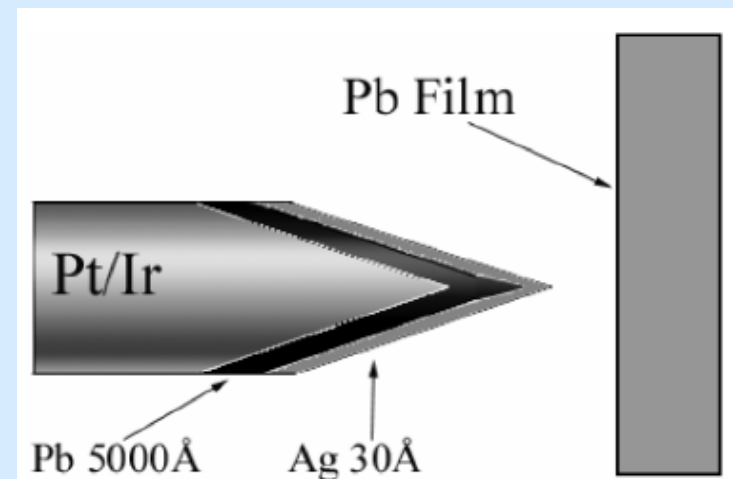
Department of Physics, University of California, San Diego, 9500 Gilman Drive, La Jolla, California 92093-0319

(Received 9 March 2001; published 14 August 2001)

We demonstrate Josephson tunneling in vacuum tunnel junctions formed between a superconducting scanning tunneling microscope tip and a Pb film, for junction resistances in the range 50–300 k Ω . We show that the superconducting phase dynamics is dominated by thermal fluctuations, and that the Josephson current appears as a peak centered at small finite voltage. In the presence of microwave fields ($f = 15.0$ GHz) the peak decreases in magnitude and shifts to higher voltages with increasing rf power,

ing tips have been demonstrated in the past [2], all STM studies so far have been performed using normal-metal tips, thus probing only the single-particle excitation spectrum, the gap structure which is a consequence of superconductivity, but not the superconducting (SC) ground state itself. Results from STM measurements of HTSC

resistances of 50–300 k Ω , and demonstrate that this is due to Cooper pair tunneling by considering both the dc and ac Josephson effects in the presence of strong thermal fluctu-



Subgap structure in asymmetric superconducting tunnel junctions

Markus Ternes,^{1,*} Wolf-Dieter Schneider,¹ Juan-Carlos Cuevas,² Christopher P. Lutz,³
Cyrus F. Hirjibehedin,³ and Andreas J. Heinrich³

¹*Institut de Physique des Nanostructures, École Polytechnique Fédérale de Lausanne, CH-1015 Lausanne, Switzerland*

²*Institut für Theoretische Festkörperphysik, Universität Karlsruhe, D-76128 Karlsruhe, Germany*

³*IBM Research Division, Almaden Research Center, 650 Harry Road, San Jose, California 95120, USA*

(Received 13 September 2005; published 2 October 2006)

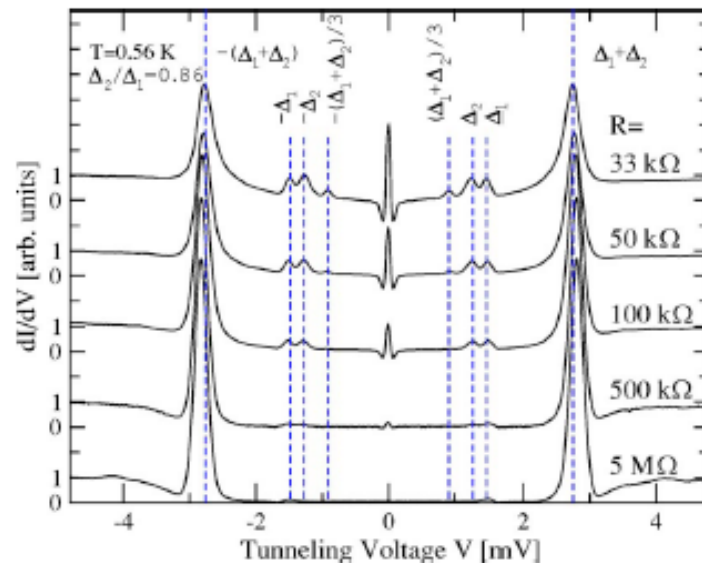
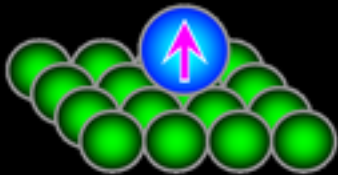


FIG. 1. (Color online) dI/dV spectra observed at 0.56 K between a superconducting sample and tip with nearly equal gaps ($\Delta_1=1.47$ meV, $\Delta_2=1.27$ meV) showing Andreev reflections for different junction resistances. All spectra are normalized by R . The peak evolving at $V=0$ is due to the Josephson supercurrent. The dotted lines are a guide for the eye marking characteristic features in the spectra. The spectra are shifted vertically with respect to each other for better visibility.

$100\mu\text{V} \approx 48 \text{ GHz}$

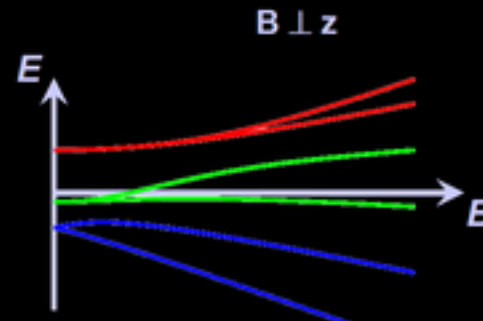
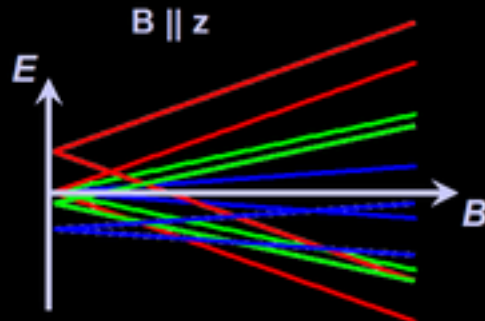
Magnetic Anisotropy

Anisotropy at a surface



- Free atomic spin is rotationally invariant: all spin orientations are degenerate.
- Loss of rotational symmetry breaks degeneracy of spin orientations.

$$H = -g\mu_B \vec{B} \cdot \vec{S} + DS_z^2$$



Magnetic field dependence varies with angle of magnetic field.

Cyrus F. Hirjibehedin, Chiung-Yuan Lin, Alexander F. Otte, Markus Ternes, Christopher P. Lutz, Barbara A. Jones, and Andreas J. Heinrich, "Large Magnetic Anisotropy of a Single Atomic Spin Embedded in a Surface Molecular Network," *Science* **317**, 1199 (2007).

Spin Excitations of a Kondo-Screened Atom Coupled to a Second Magnetic Atom

A. F. Otte,^{1,2,*} M. Ternes,^{1,3} S. Loth,^{1,4} C. P. Lutz,¹ C. F. Hirjibehedin,^{1,5} and A. J. Heinrich^{1,†}¹IBM Research Division, Almaden Research Center, San Jose, California 95120, USA²Kamerlingh Onnes Laboratorium, Universiteit Leiden, 2300 RA Leiden, The Netherlands³Max-Planck-Institut für Festkörperforschung, Heisenbergstrasse 1, 70569 Stuttgart, Germany⁴Department of Physics, University of California at Berkeley, Berkeley, California 94720, USA⁵London Centre for Nanotechnology, Department of Physics and Astronomy, Department of Chemistry, University College London,

PRL 103, 107203 (2009)

PHYSICAL REVIEW LETTERS

week ending
4 SEPTEMBER 2009

$$\hat{\mathcal{H}} = J\hat{\mathbf{S}}^{(\text{Fe})} \cdot \hat{\mathbf{S}}^{(\text{Co})} - \mu_B \mathbf{B} \cdot (g_{\text{Fe}}\hat{\mathbf{S}}^{(\text{Fe})} + g_{\text{Co}}\hat{\mathbf{S}}^{(\text{Co})}) \\ + D_{\text{Fe}}\hat{S}_x^{2(\text{Fe})} + E_{\text{Fe}}(\hat{S}_y^{2(\text{Fe})} - \hat{S}_z^{2(\text{Fe})}) + D_{\text{Co}}\hat{S}_y^{2(\text{Co})}. \quad (1)$$

The first term represents an isotropic Heisenberg coupling between the spins $\hat{\mathbf{S}}^{(\text{Fe})}$ on the Fe atom and $\hat{\mathbf{S}}^{(\text{Co})}$ on the Co atom, quantified by the Heisenberg exchange coupling strength J . According to this definition, positive values of J signify antiferromagnetic coupling. The second term gives the Zeeman energies resulting from the external magnetic field \mathbf{B} , where μ_B denotes the Bohr magneton and g_{Fe} and g_{Co} the g factors of the Fe and Co spins, respectively.

The remaining terms in Eq. (1) represent the magneto-crystalline anisotropies experienced by each of the spins, quantified by the uniaxial anisotropy parameters D_{Fe} and D_{Co} and the transverse anisotropy parameter E_{Fe} . All parameters in this spin Hamiltonian except J have been measured previously on the corresponding isolated atoms. The choice of spin magnitudes, $S_{\text{Fe}} = 2$ and $S_{\text{Co}} = 3/2$, the assignment of the axes in the anisotropy terms, and the absence of transverse anisotropy for Co are based on previous studies of the isolated atoms on the same surface [10,17].

Diagonalization of the spin Hamiltonian gives a system of 20 eigenstates with corresponding eigenenergies [24]. To determine which of the excited states are accessible through inelastic excitations by the tunneling electrons we use an excitation intensity model as employed in [17]. Here we extend this model to include the effect of the tip position by using only the spin operators for the atom probed by the tip:

$$I_{0 \rightarrow n}^{(\text{Co})} = |\langle \psi_n | \hat{S}_x^{(\text{Co})} | \psi_0 \rangle|^2 + |\langle \psi_n | \hat{S}_y^{(\text{Co})} | \psi_0 \rangle|^2 \\ + |\langle \psi_n | \hat{S}_z^{(\text{Co})} | \psi_0 \rangle|^2. \quad (2)$$

Here $I_{0 \rightarrow n}^{(\text{Co})}$ is the transition intensity from the ground state

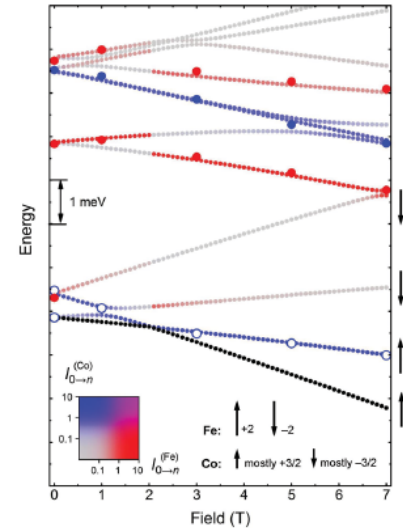


FIG. 3 (color). Small dots: lowest 12 eigenvalues of Eq. (1) with $J = 0.13$ meV, $g_{\text{Fe}} = 2.11$, $g_{\text{Co}} = 2.16$, $D_{\text{Fe}} = -1.53$ meV, $E_{\text{Fe}} = 0.31$ meV and $D_{\text{Co}} = 2.70$ meV for $B = 0$ to 7 T in increments of 0.1 T along x . Color indicates the values of $I_{0 \rightarrow n}^{(\text{Co})}$ (blue) and $I_{0 \rightarrow n}^{(\text{Fe})}$ (red) as indicated by the color key on the left. The ground state is colored black. Large dots: experimental data points indicating positions of peaks (open circles) and steps (filled circles) in Figs. 2(a) (blue, Co) and 2(c) (red, Fe), all plotted relative to the calculated ground state. The zero of the energy axis is arbitrary, as only energy differences between states are observable. Arrows indicate the magnetization along the x direction of the Co spin (short arrows) and the Fe spin (long arrows) for the four lowest-energy states. This labeling also applies at low fields, as if the avoided crossing near 1 T were a true crossing. At the ground-state level crossing at 2.1 T, only the Co spin changes direction.

LT - STM using the ac-Josephson Effect

Klaus Baberschke

Institut für Experimentalphysik, Freie Universität Berlin,

Arnimallee 14, D-14195 Berlin, Germany

In the past a voltage biased point contact of an SIS junction has been used to create an electromagnetic ac-field, i. e. the ac-Josephson effect. The linear relation between voltage and frequency $h\nu = 2eV$ provides a wide range of frequencies, between $\sim 10^8 - 10^{13}$ Hz. The dissipation of energy can be detected in the I-V curve /1/.

In this lecture we propose to combine this with today's LT-STM technique. This will be a combination of early days point contact spectroscopy with today's STM of atomic resolution. It will open a new field of spectroscopy to investigate atoms, molecules, single molecular magnets, etc. on surfaces and surface magnetism. In the past, mostly inelastic electron tunnelling spectroscopy (IETS) was used. Here we propose to generate an electromagnetic ac-field. This can be used to measure, by means of M1 and E1 transitions, the low energy eigenstates of the crystal field splitting of magnetic ions, see for example Fig. 3 in /2/.

Another way to create electromagnetic fields over a large range in frequency is to use synchrotron radiation. We will comment on recent experiments at BESSY.

/1/ K. Baberschke et al. Phys. Rev. Lett. 53, 98 (1984).

/2/ A. F. Otte et al. Phys. Rev. Lett. 103, 107203 (2009)

IBM June 9. 2010